Environmental Science Processes & Impacts

ROYAL SOCIETY OF CHEMISTRY

PAPER

View Article Online
View Journal | View Issue

Cite this: *Environ. Sci.: Processes Impacts*, 2025, **27**, 188

Modelling indoor radical chemistry during the HOMEChem campaign†

Freja F. Østerstrøm, ‡§[a] Toby J. Carter, §[a] David R. Shaw, [a] Jonathan P. D. Abbatt, [b] Andrew Abeleira,[c] Caleb Arata,[de] Brandon P. Bottorff, [f] Felipe J. Cardoso-Saldaña, [g] Peter F. DeCarlo, [h] Delphine K. Farmer, [c] Allen H. Goldstein, [ei] Lea Hildebrandt Ruiz, [g] Tara F. Kahan, [jk] James M. Mattila, [c] Atila Novoselac,[l] Philip S. Stevens, [fm] Emily Reidy,[f] Colleen Marciel F. Rosales, [m] Chen Wang, [b] Shan Zhou[jn] and Nicola Carslaw *[a]

In the indoor environment, occupants are exposed to air pollutants originating from continuous indoor sources and exchange with the outdoor air, with the highest concentration episodes dominated by activities performed indoors such as cooking and cleaning. Here we use the INdoor CHEMical model in Python (INCHEM-Py) constrained by measurements from the House Observations of Microbial and Environmental Chemistry (HOMEChem) campaign, to investigate the impact of a bleach cleaning event and cooking on indoor air chemistry. Measurements of the concentrations of longer-lived organic and inorganic compounds, as well as measured photolysis rates, have been used as input for the model, and the modelled hydroxyl (OH) radicals, hydroperoxyl (HO_2^*) radicals, and nitrous acid (HONO) concentrations compared to the measured values. The peak modelled OH, HO_2^*, and HONO concentrations during cooking and cleaning activities are about 30%, 10%, and 30% higher than the observations, respectively, within experimental uncertainties. We have determined rates for the rapid loss of HONO formed through cooking activities onto a wet surface during the cleaning events and also for the subsequent slow release of HONO from the cleaned surface back into the gas-phase. Using INCHEM-Py we have also predicted peak concentrations of chlorine (Cl) atoms, (0.75–2.3) × 10^5 atom per cm^3 at the time of cleaning. Model predictions of the Cl atom and OH radical reactivities were also explored, showing high Cl atom reactivity throughout the day, peaking around 5000–9000 s^{-1}. The OH reactivity was found to increase from a background value close to urban outdoor levels of 20–40 s^{-1}, to levels exceeding observations in outdoor polluted areas following cooking and cleaning activities (up to 160 s^{-1}). This underlines the high oxidation capacity of the indoor atmospheric environment through determining the abundance of volatile organic compounds.

Received 18th October 2024
Accepted 9th December 2024

DOI: 10.1039/d4em00628c

rsc.li/espi

[a]*Department of Environment and Geography, University of York, York, UK. E-mail: nicola.carslaw@york.ac.uk*
[b]*Department of Chemistry, University of Toronto, Toronto, Canada*
[c]*Department of Chemistry, Colorado State University, Fort Collins, CO, USA*
[d]*Department of Chemistry, University of California Berkeley, Berkeley, CA, USA*
[e]*Department of Environmental Science, Policy and Management, University of California Berkeley, Berkeley, CA, USA*
[f]*Department of Chemistry, Indiana University Bloomington, Bloomington, IN, USA*
[g]*McKetta Department of Chemical Engineering, University of Texas at Austin, Austin, TX, USA*
[h]*Department of Environmental Health and Engineering, Johns Hopkins University, Baltimore, MD, USA*
[i]*Department of Civil and Environmental Engineering, University of California Berkeley, Berkeley, CA, USA*
[j]*Department of Chemistry, Syracuse University, Syracuse, NY, USA*
[k]*Department of Chemistry, University of Saskatchewan, Saskatoon, Canada*
[l]*Department of Civil, Architectural, and Environmental Engineering, University of Texas at Austin, Austin, TX, USA*
[m]*O'Neill School of Public and Environmental Affairs, Indiana University Bloomington, Bloomington, IN, USA*
[n]*Department of Civil and Environmental Engineering, Rice University, Houston, TX, USA*

† Electronic supplementary information (ESI) available. See DOI: https://doi.org/10.1039/d4em00628c

‡ Now at: Department of Environmental Science, Aarhus University, Roskilde, Denmark.

§ These authors contributed equally to this work.

Environmental significance

Cooking and cleaning are sources of radical species, which can react to form potentially harmful secondary pollutants indoors. This paper aims to investigate indoor air chemistry following cooking and cleaning. Air pollutant measurements during the HOMEChem campaign have been used to constrain an explicitly detailed indoor air chemistry model, INCHEM-Py. We show that indoor radical concentrations following cleaning can be 15–20 times higher than those typically observed outdoors, enhancing oxidation of volatile organic compounds. We also show that nitrous acid formed through cooking, behaves differently on wet and dry surfaces, being held on wet surfaces before slowly off-gassing as the floor dries. In short, cooking and cleaning can have a major impact on reactivity in a typical residential environment.

1 Introduction

Air pollution has become one of the biggest challenges in the 21st century, with exposure to air pollutants considered to be one of the greatest risks to global human health.[1] According to the World Health Organisation (WHO), 6.7 million premature deaths per year were attributed to exposure to air pollutants in 2020, with 3.2 million deaths arising from exposure to household air pollution caused by solid fuel burning in less developed countries.[2] In fact, the WHO recently stated that improving air quality would reduce the global incidence and impact of numerous diseases, such as lung cancer, stroke and asthma.[1] Indoor air quality became even more important with the recent COVID-19 pandemic and highlighted the possibility of viral transmissions indoors. Such issues have led to calls for indoor air to be regulated, at least in public places.[3,4]

In developed countries, 90% of our time is spent indoors, with roughly two thirds of our time in our homes.[5] Consequently, most of our exposure to air pollutants happens indoors, even if these pollutants were generated outdoors originally. Outdoor air pollutants are able to enter buildings through windows, doors, and cracks in the building envelope, as well as *via* mechanical ventilation. Once indoors, they combine with indoor emissions to form a complex chemical mixture, about which relatively little is known. However, there is evidence that some of the reaction products of this chemical mixture are harmful to health.[6]

There are numerous air pollutants indoors from a range of sources. For instance, a comprehensive review of the literature identified nearly 900 unique chemical species that had been measured in indoor air.[7] Understanding which of these pollutants is most important in terms of health effects and then linking them to their dominant sources, is crucial to advance the science and mitigate accordingly, but remains a challenge. There are numerous sources of air pollutants in typical homes, including building materials (*e.g.*, plasterboard, timber), furnishing and decorative materials (*e.g.*, flooring materials, paints), occupant activities (*e.g.*, cooking and cleaning), as well as from outdoors.[8] Emissions of air pollutants from buildings, furnishing and decorative materials tend to be highest from new materials and dominated by volatile organic compounds (VOCs).[9–12]

Occupant emissions can be further divided into (a) passive, from skin and breath emissions, including squalene, fatty acids, carbon dioxide, acetone, nitric oxide, ammonia and isoprene[13,14] and (b) active, from activities such as cooking, cleaning, air freshener use, and including VOCs, nitrous acid, nitrogen oxides, ammonia, chlorinated compounds and particulate matter.[6,15,16] Pollutants that are derived from outdoors depend on the building location and typically comprise of ozone, VOCs, nitrogen oxides and particulate matter, the latter two particularly near to transport emissions. These sources will vary in strength, over time, with ventilation, and by building. Furthermore, the sources will also interact with each other.

Indoor air quality science has advanced significantly in recent years, largely through adapting outdoor air pollutant instrumentation for use indoors, and undertaking advanced laboratory, chamber, test-house and modelling studies.[17–20] These studies have demonstrated the chemical diversity of the indoor environment, particularly during typical activities such as cooking[21–32] or cleaning.[23,24,31–35] The importance of surfaces indoors has also been highlighted. Surface area to volume ratios (A/V) are much higher indoors (3 m^{-1}) than outdoors (10^{-3} to 10^{-2} m^{-1}),[36] and surfaces can act as both sinks and sources of indoor air pollutants.[37–39]

One of the most detailed indoor air chemistry studies to date, was the House Observations of Microbial and Environmental Chemistry (HOMEChem) campaign. HOMEChem was carried out in June 2018 at the University of Texas at Austin's test house (the UTest House) in Austin, Texas, USA, and involved 13 universities.[17] Typical indoor activities were simulated during the course of the campaign, including cooking and cleaning events, as well as simulating a mixture of cooking and cleaning. A huge suite of measurements were made during these activities. These included the physical parameters of the house, such as temperature and pressure, as well as a comprehensive chemical characterisation, including VOCs, chloroorganic compounds, particles, nitrogen oxide species (NO_x; nitric oxide (NO) + nitrogen dioxide (NO_2)), ozone (O_3), photolysis rates, hydroxyl (OH) and hydroperoxyl (HO_2) radicals, and nitrous acid (HONO).[17]

From the experimental activities performed during HOMEChem, Reidy *et al.* (2023),[40] found that OH was a chemical signature of cooking. The study found that OH increased from $\approx 1 \times 10^6$ molecule per cm^3 to $\approx 6 \times 10^6$ molecule per cm^3 over the course of 3 hours during a Thanksgiving-type cooking period (performed on June 27), whilst four people were present. Following the cooking, the occupancy of the room increased to 13 people, and the OH concentration decreased to $\approx 1.5 \times 10^6$ molecule per cm^3.[40] According to Zannoni *et al.* (2022),[41] when concentrations of ozone are low indoors, radical sinks can arise in the form of people, clothing and skin surfaces. For instance, once everybody had vacated the room following the Thanksgiving dinner, the OH concentration returned to $\approx 6 \times 10^6$ molecule per cm^3, as the radical sinks were removed.[40] A goal of

this paper is build upon the Reidy *et al.* (2023) study[40] by modelling indoor radical chemistry not only from cooking but also from cleaning. OH and Cl reactivities can also be modelled to provide an insight into indoor oxidation capacities during and after occupational activity.

Further research from HOMEChem included a study by Wang *et al.* (2022)[32] who found that bleach cleaning (chlorine-based cleaning) and cooking were key sources of indoor isocyanic acid (HNCO), which is known to cause a multitude of health effects.[42] This was the first study to have categorised a link from indoor, occupancy-led activities to HNCO. It was found that HNCO mixing ratios were regulated by surface–air interactions and partitioning. Wang *et al.* (2022)[32] found average HNCO mixing ratios of 0.14 ppb indoors, compared to an average of 0.026 ppb outdoors, indicating an occupancy-led formation of these nitrogen-containing gases.

HONO is also an important component in indoor air as it is a precursor to OH radicals and has direct health impacts.[43–45] However, predicting indoor (and outdoor) concentrations of HONO have been challenging.[43,46,47] Collins *et al.* (2018)[48] found evidence of a gas-surface equilibrium mechanism for HONO, enhancing the previously understood surface reaction of NO_2. HONO concentrations were found to be strongly controlled by this gas-surface equilibrium mechanism. Surface reservoirs and multi-phase mechanisms have been found to dominate many gas-surface processes of indoor air constituents, influencing concentrations of HONO among other species following different indoor activities.[33,49]

Whilst an increasing number of indoor air measurements have been performed in recent years, the complexity of indoor environments makes them a challenging system to describe. Indoor air chemistry models are good tools to understand the chemistry in the absence of observational data or to provide further insight when used alongside measurements. The INdoor CHEMical model in Python (INCHEM-Py) has been optimised for increasing our understanding of chemical processing in indoor environments.[50,51] The model has been used to investigate indoor air quality following cooking,[25] cleaning,[34,52–59] surface emissions,[38,39,60–62] skin and breath emissions from occupants,[13] effects on outdoor air from indoor emissions,[63] indoor photolysis reactions[64,65] and particle formation through chemistry.[66–68] In this study, we have used INCHEM-Py to probe radical chemistry during the HOMEChem campaign.

We have selected four so-called layered days for study, June 8, 19, 21, and 25, during which several different types of cleaning and cooking events were performed. The layered days during the campaign aimed to simulate a combination of activities that would be carried out in a typical house over the course of a day. Each day is comprised of three cooking events (breakfast, lunch, and dinner), followed by different types of cleaning events (clorox wipes, pine sol cleaning, and bleach cleaning). It should be noted that a gas stove is used for the cooking activities, NO_x conditions would therefore be much different if the cooking were done on an electric range. The focus of this study is on the bleach cleaning (Cl-cleaning) event that takes place around 17:35 local time and lasts 10 minutes on each of the layered days. Using the measured VOCs, chlorine-containing compounds, NO_x, O_3, H_2O, photolysis rates, and physical parameters as model inputs, we compare measured and modelled OH and peroxy radicals, as well as HONO concentrations. The model is also used to predict chlorine (Cl) atom concentrations and to calculate OH and Cl reactivity (none of which were measured) following bleach cleaning. June 25 is used as a detailed case study day, but we also use an idealised averaged day based on input data from all four days.

2 Methods

2.1 The INdoor CHEMical model in Python (INCHEM-Py)

The INdoor CHEMical model in Python (INCHEM-Py)[50,51] describes indoor atmospheric chemistry using the Master Chemical Mechanism v. 3.3.1 (MCM),[69,70] and several additional reaction schemes specifically designed for indoor processes. The MCM is a near-explicit mechanism that considers the degradation of ~140 VOCS in the atmosphere. Depending on their structure, the VOCs can initially react with ozone, OH, the nitrate radical, or undergo photolysis. These preliminary steps produce a range of radical species, which can, in theory, undergo further oxidation steps until the final products of water and carbon dioxide are formed. We have also included a chlorine chemistry scheme, based on Xue *et al.* (2015),[71] which includes VOC reactions with Cl atoms, meaning INCHEM-Py can track and predict the concentrations of HOCl and Cl_2 among other key indoor chlorine-containing species. Photolysis rate coefficients of Cl_2, $ClNO_2$, $ClONO_2$, HOCl, OClO, ClO and ClO_2Cl are also included in the model.[65] A new HONO gas-surface chemical scheme based on Collins *et al.* (2018)[48] has also been used in this study. The total mechanism consists of over ~17 000 reactions and over ~6000 species.[69,70,72–75] As well as gas-phase chemistry, the model also considers the formation of secondary organic aerosols (SOA) for limonene, alpha- and beta-pinene;[66,68] surface deposition and subsequent product emission for ozone and hydrogen peroxide;[38] indoor–outdoor exchange of all gas and particle species; and wavelength dependent photolysis from both attenuated outdoor and indoor light sources.[65] The sensitivity of model outputs to the input parameters as well as the 95% confidence bounds for our predicted concentrations was provided by Kruza *et al.* (2021),[61] using an earlier version of the model.

Two major modifications to the model are employed for this work: (1) constraining long-lived species concentrations, physical parameters (temperature and relative humidity) and selected photolysis rates to measured values. The constrained parameters are listed in Table S1 in the ESI.† Breath emissions were also added according to the number of occupants as described in Kruza and Carslaw (2019).[13] All remaining species and photolysis rates are calculated as described in Wang *et al.* (2022)[65] and Shaw *et al.* (2023).[51] (2) Addition of a HONO surface chemistry scheme, specifically for treating the impact of the wet bleach-covered surface and subsequent degassing on HONO concentrations, during and after the bleach cleaning events. The HONO surface chemistry reactions described by Collins *et al.* (2018)[48] formed the basis of this scheme, with additional

surface reactions added to better capture the cleaning episode (see Section 2.5).

2.2 Preprocessing of HOMEChem data for model input

The measured concentrations of 45 indoor VOCs, 6 indoor inorganic chlorine and chloroorganic compounds (Cl-compounds), indoor and outdoor O_3 and NO_x concentrations, as well as 11 measured indoor photolysis rates, temperature, indoor water concentrations and air change rates, were used to initialise the model,[76] as shown in Table 1, which shows that these measurements were made by multiple instruments. Data from the four layered days of the campaign were used, namely June 8, 19, 21, and 25, 2018. The events on these days consisted of cooking and cleaning, simulating everyday activities in a house. The focus of this study is on the Cl-cleaning events taking place on each of the four days around 17:35–17:45 local time. For each of these events, 120 mL of bleach was mixed in 3.8 L of tap water, although the mass of bleach solution used on each of these days varied (196, 455, 1522 and 1476 g on June 8, 19, 21, and 25 respectively). Two sets of model runs were performed: (1) using the input data for June 25 and (2) using an average input of all four days.

The raw measured data from each instrument was provided at varying intervals, from per second to per minute, and started at different time points. For each layered day, all null values and values logged as lower than the detection limit of the specific instrument were first removed. To fill in data gaps, a linear interpolation was used, with data points at either 1 second or 1 minute frequency depending on the frequency of the original data. An exponential moving average at the required interval (5- or 15 minutes) was then calculated at each time point. This process allowed us to use longer time intervals for most of the day, with 5 minutes intervals focused around the cleaning event in the evening, when concentrations tended to change more rapidly. Two datasets were then produced, one for June 25, and one that averaged the four layered days (June 8, 19, 21, and 25, 2018). Additional indoor and outdoor species that are not input into the model are initiated based on previous indoor/outdoor observations and assumptions as described in Carslaw *et al.* (2007),[84] Shaw *et al.* (2021),[50] and Shaw *et al.* (2023).[51] The outdoor concentration of HONO was initialised at 0.65 ppb.[85] Although outdoor HONO was measured during the campaign, measurements are sporadic and not always available for the days we focussed on. The literature value agrees well with outdoor HONO concentrations measured on other days during HOMEChem.[24] There were no measurement data available for molecular chlorine (Cl_2), hypochlorous acid (HOCl), chloroformic acid ($ClCO_2H$), chlorine nitrite ($ClNO_2$) or the photolysis rates of J_{ClOOCl} (J77) and J_{OClO} (J75) for June 21, so the average day constitutes average values for June 8, 19 and 25 for these inputs.

2.3 Physical parameters and occupancy

INCHEM-Py simulated a single well-mixed environment representing the UTest House with an A/V ratio of 1.78 m^{-1}. Using surface data from previous studies, individual surface area-to-

Table 1 Instruments used during HOMEChem to measure the different species and rates inputted in the model, or used for comparison to model output

Species	Instrument	Institution and references	Notes
HONO	Acetate CIMS	University of Toronto[24,49,77]	Compared to model output and Indiana University Bloomington measurements of HONO
OH, HO_2, HO_2^*, HONO	LIF-FAGE	Indiana University Bloomington[40,78]	Not inputted, but used for comparison to model output
Isoprene, benzene, toluene, Methyl Vinyl Ketone (MVK)	PTR-TOF-MS	University of California Berkeley[23,79]	All four compounds: used the average values for entire campaign in the model initialisation
VOCs	GC	Colorado State University[80]	MVK is not input, trichloromethane and tetrachloroethane was measured with this instrument
Cl-compounds	Iodide CIMS	Colorado State University[81]	
O_3, $O_{3,out}$	Ambient ozone monitor	Colorado State University[17]	
NO, NO_{out}, $NO_{2,out}$	Model 42i-D nitrogen oxide NO_x analyzer	Colorado State University[17]	
NO_2	CAPS	University of Texas at Austin[17,82]	
CO, CH_4	Picarro CRDS	Johns Hopkins University[83]	
Photolysis rates	Ocean optics spectrometer	University of Saskatchewan[76]	Living room measurements used as they were adjacent to LIF-FAGE instrument
T, H_2O, air change	Varying sensors in house	University of Texas at Austin[17]	H_2O calculated from relative humidity measurement. Air change is kept constant in the model
Occupancy, lights on/off	Activity log	Colorado State University[17]	Recorded by HOMEChem participants

volume ratios for a range of different indoor surface materials were simulated.[38,63,86] This enables ozone and hydrogen peroxide deposition to occur, followed by the subsequent emission of secondary pollutants following surface transformations.[38] The simulated kitchen was assumed to be comprised of; soft furnishings (0.05 m^{-1}), painted surfaces (0.66 m^{-1}), wood (0.44 m^{-1}), metal (0.21 m^{-1}), concrete (0.03 m^{-1}), paper (0.01 m^{-1}), plastic (0.19 m^{-1}), glass (0.04 m^{-1}) and the skin surface of three adults (0.16 m^{-1} when occupied). The total volume of the house (V) is 250 m^3 and the floor area (the area that was cleaned during the Cl-cleaning events) is 40 m^2 (A_{clean}). On June 25, three adults were in the room from 08:25 to 17:55 resulting in breath emission rates as described in Kruza *et al.* (2019).[13] The same occupancy patterns and cleaning times were used for both the case study and the average day simulations. The air change rate was 0.59 h^{-1} for June 25 and 0.5 h^{-1} for the averaged day.

2.4 Photolysis rates

There was one spectrophotometer deployed during the HOMEChem campaign, so photolysis rates were only measured in one room at a time. The instrument was therefore moved occasionally between the eastward facing kitchen and the westward facing living room. Consequently, the average diurnal profile adopted a bimodal shape as light entered the house from either the living room or kitchen window.[76] These spectral measurements were taken close to the windows, both at the east and the west of the house, indicating that measured photolysis rates will be lower throughout most of the house. It is worth noting that the LIF instrument was located closed to the west window. Eleven photolysis rate coefficients were measured during the campaign[76] as detailed in Table S1.† Eastward facing photolysis rates were highest before 15:14, after which westward facing rates began to dominate.[76] Photolysis rates from June 5–9, 11–16, and 18–27, were averaged to 5- or 15 minutes intervals as described in Section 2.2, and incorporated into the model for both June 25 and the averaged layered day scenarios. We used campaign averaged photolysis rates due to a lack of data from individual days, and variation in weather patterns (*e.g.*, cloud cover). Fig. 1 shows five representative photolysis rate coefficients used as inputs in the model: $J_{NO_3\rightarrow NO}$, $J_{NO_3\rightarrow NO_2}$, J_{NO_2}, J_{HONO}, and J_{Cl_2}. The remaining outdoor photolysis rates, attenuated through the windows, and the contribution from artificial lighting indoors were calculated as described by Wang *et al.* (2022).[65] These were based on assuming low emissivity glass and incandescent indoor lighting. The lights of the building were on when occupants were present, however, attenuated outdoor photolysis is expected to drive indoor photochemistry on this photochemically active day.

2.5 HONO surface chemistry

The chemical scheme from Collins *et al.* (2018)[48] describing a surface reaction of NO_2 to produce gas-phase HONO, combined with the subsequent gas-surface HONO equilibrium is summarised in reactions ((1)–(3)). Reactions (2) and (3) were the main drivers of the indoor steady state HONO

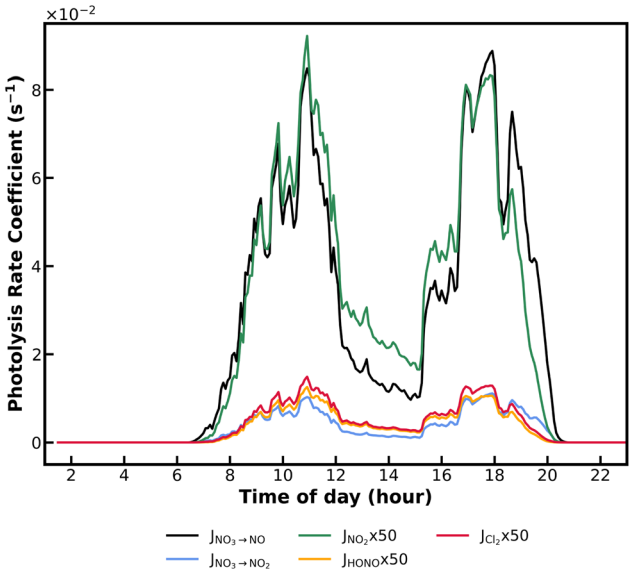

Fig. 1 Selected average photolysis rate coefficients (J) from measurements located both in the kitchen and living room, representing the outdoor attenuated light experienced inside the house: $J_{NO_3\rightarrow NO}$ (black line), $J_{NO_3\rightarrow NO_2}$ (blue line), J_{NO_2} × 50 (green line), J_{HONO} × 50 (yellow line), and J_{Cl_2} × 50 (red line).

concentration, where the surface acts as a reservoir of nitrite and HONO that is in equilibrium with the gas-phase through the two reactions. When accounting for the A/V ratio of the indoor environment in their study, the reactions and their rate coefficients (k) can be generalised to depend on the A/V ratio in any environment thus:

$$\begin{aligned} &NO_2(g) \rightarrow HONO(g) \\ &k_1 = 7.00 \times 10^{-3}\ \text{cm s}^{-1} \times A/V \end{aligned} \quad (1)$$

$$\begin{aligned} &HONO(g) \rightarrow \text{surface} \\ &k_2 = 5.67 \times 10^{-2}\ \text{cm s}^{-1} \times A/V \end{aligned} \quad (2)$$

$$\begin{aligned} &\text{surface} \rightarrow HONO(g) \\ &k_3 = 1.33 \times 10^{10}\ \text{molecule cm}^{-2}\ \text{s}^{-1} \times A/V \end{aligned} \quad (3)$$

The Collins *et al.* (2018)[48] mechanism (reaction (1)–(3)) was added into the INCHEM-Py model throughout the simulations, utilising the A/V of the UTest House (1.78 m^{-1}). The mechanism applies to the dry surfaces of the house, and was represented using reactions (1)–(3) in the chemical mechanism in the model. However, the HONO equilibrium with the surfaces changes drastically when the floor is wet during cleaning, as well as the following period when the floor was drying. The surface chemistry in INCHEM-Py was modified to account for this change, using the measurements from June 25. We assumed there were two processes: (1) HONO uptake onto wet surfaces and (2) HONO slowly degassing from the cleaned surface/reaching steady state concentration in the air after the cleaning event.

$$\text{HONO (g)} \rightarrow \text{HONO (wet surface)} \quad (4)$$

$$\text{HONO (wet surface)} \rightarrow \text{HONO (g)} \quad (5)$$

Reactions (4) and (5) are only activated in the model at the time of cleaning and until HONO reaches a steady state between gas and surfaces afterwards. We assumed the floor was wet (fully and partially) between 17:35–18:25, activating reaction (4). The drying and degassing process of reaction (5) was activated in the model between 17:50–22:00. The fitted rates for these reactions are included in the Results and discussion (Section 3).

2.6 HO_2^*

The laser-induced fluorescence technique fluorescence assay by gas expansion (LIF-FAGE) measurement technique was used to measure OH and HO_2 radicals. However, the technique can suffer from known interference from reactions of OH with alkenes within the instrument, which produce organic peroxy radicals (RO_2), which subsequently react with NO to form HO_2 radicals. Subsequently, the LIF-FAGE HO_2 measurements actually represent HO_2 plus some of the RO_2 present in the sampled air.[40,87] Due to this interference, a new parameter was created in the model called HO_2^*, which is a summation of HO_2 and a selection of RO_2 species derived from OH-oxidation. The OH derived oxidative species included in the HO_2^* summation are HO_2 radicals, seven isoprene-derived RO_2 radicals, nine monoterpene-derived RO_2 radicals, the methylperoxy radical (CH_3O_2), the acetylperoxy radical (CH_3CO_3), one ethene-derived RO_2 radical and two propane-derived RO_2 radicals. These particular species are included in the HO_2^* summation, because the VOCs which derived these RO_2 species had high concentrations during the cooking and cleaning events, therefore are key to the overall sum of RO_2 species. It was not necessary to include every single RO_2 species because most had negligible concentrations.

3 Results and discussion

3.1 Model *versus* measured comparisons

Fig. 2 shows a comparison of modelled *versus* measured concentrations of OH radicals (panel a), HO_2^* radicals (panel b), and HONO (panel c) on June 25, 2018. Cooking and cleaning activities are indicated by the shaded areas and experimental uncertainties are also shown. The main peaks in OH (panel a) and HO_2^* (panel b) radicals are observed at the time of Cl-cleaning (17:35–17:45). The measured OH radicals are influenced early in the day by an overnight ozone experiment carried out in the house. Modelled HO_2^* shows excellent agreement with the measured HO_2^* for the entire day. The three major peaks in both measured and modelled HONO (panel c) correspond to the cooking events (with a gas stove). The sudden decrease in HONO observed at the time of Cl-cleaning is followed by a slow recovery. All three species show excellent agreement between the modelled and measured values within the experimental uncertainties.

Fig. 3 shows model output for the averaged day input (black line) for OH radicals (panel a) and HONO (panel b) *versus* the available measurements for each species for the four layered

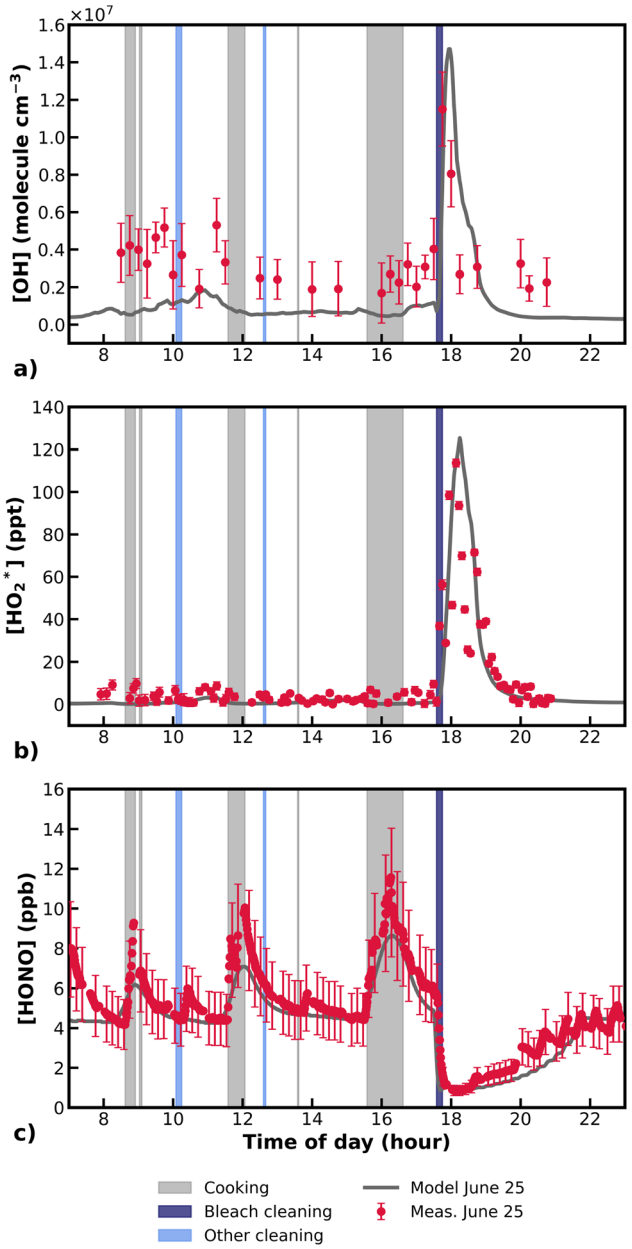

Fig. 2 Modelled (grey line) *versus* measured (red circles) concentrations of OH radicals (panel a, molecule per cm^3), HO_2^* radicals (panel b, ppt), and HONO (panel c, ppb) on June 25. Error bars represent the experimental uncertainties. The shaded areas indicate the timing of the activities carried out during the day: cooking (grey), Cl-cleaning (dark blue), and other cleaning (light blue) activities.

days (coloured symbols). The agreement between modelled and measured OH radicals for the averaged day is within the experimental uncertainties at the time of the Cl-cleaning event. The cleaning peak is captured in the model, with the background OH radical concentration being lower in the model compared to the measurements. For HONO concentrations, the best agreement is with the June 8 and 25 data. The background HONO for June 19 and 21 are higher than for the other two days, particularly during the cooking events. This is because these events occurred soon after the Thanksgiving events took place

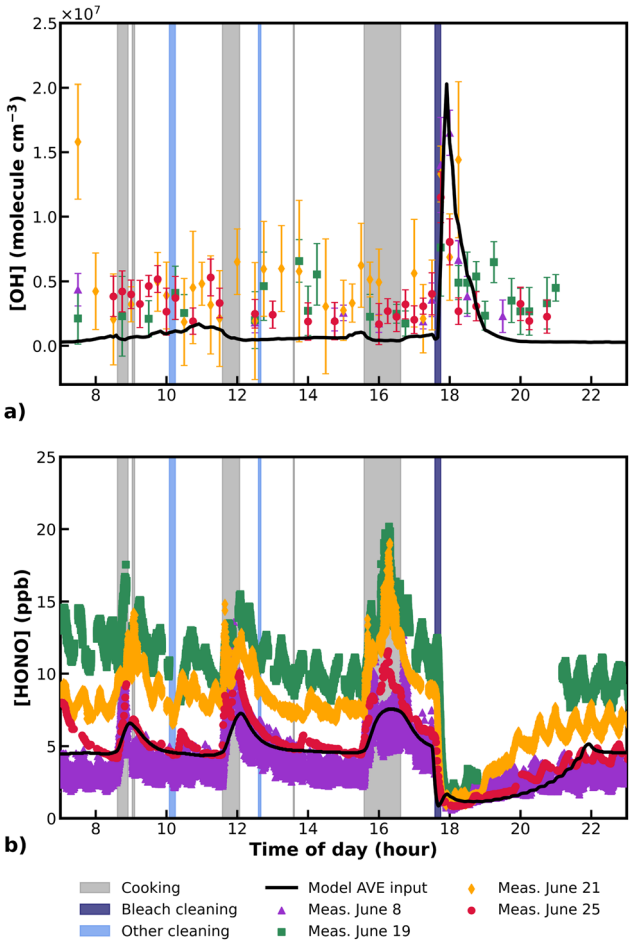

Fig. 3 Modelled averaged-day scenario concentrations (black line) of OH radicals (panel a, molecule per cm^3) and HONO (panel b, ppb) *versus* measurement concentrations (coloured symbols) of OH radicals and HONO from June 8 (purple triangles), June 19 (green squares), June 21 (yellow diamonds), and June 25 (red circles). Experimental error bars are included for the OH radical data, however they are omitted in panel b for clarity. Shaded areas indicate the timing of the indoor activities carried out: cooking (grey), Cl-cleaning (dark blue) and other cleaning (light blue) activities.

which further fuelled the importance of surface reservoirs (see Fig. 4 in Wang *et al.* (2020)[24]). The Cl-cleaning events are captured in both model scenarios.

The modelled peak values of OH on June 25 are approximately 1.5×10^7 molecule per cm^3 as seen in Fig. 2a, about 30% higher than the observations. The modelled background OH concentration is between $(0.4–1.8) \times 10^6$ molecule per cm^3, and is lower than the measured values ($(1.7–5.3) \times 10^6$ molecule per cm^3), but within their uncertainty bounds. However, for the average day (Fig. 3a) the model underestimates the background OH radical concentrations. The observed background OH radical concentrations on the four layered days are between $(2–4) \times 10^6$ molecule per cm^3, whereas the modelled background is around $(0.4–1.7) \times 10^6$ molecule per cm^3 (Fig. 2a and 3a). The use of an average of the measured photolysis rates in both model simulations (June 25 and the average day) is likely the main cause of underestimating the background concentration of OH radicals compared to the measurements. Furthermore, on the morning of June 25, an experiment was carried out including the addition of significant quantities of ozone, which may have further contributed to the underestimation of OH radical background concentrations on this day. The model to measurement agreement improves at the time of the Cl-cleaning event, with the model peak values exceeding those from the observations on the four layered days at 1.5×10^7 or 2.0×10^7 molecule per cm^3 for the June 25 and averaged-day scenario, respectively, corresponding to 1–3 times the observed OH radical concentrations; the observed peak OH radical concentrations range between $(0.8–1.7) \times 10^7$ molecule per cm^3 at the time of the Cl-cleaning event. About an hour after the Cl-cleaning event, the OH radical concentrations are back to background levels. Outdoor globally averaged concentrations of OH radicals are 1.1×10^6 molecule per cm^3.[90] The observed and modelled OH radical concentrations indoors during these events in the HOMEChem campaign are 15–20 times larger than the outdoor values, enhancing the oxidative capability of the indoor air for about an hour following the Cl-cleaning event.

The observed and modelled peak value of the HO_2^* radical summations on June 25 is approximately 127 ppt at 18:15

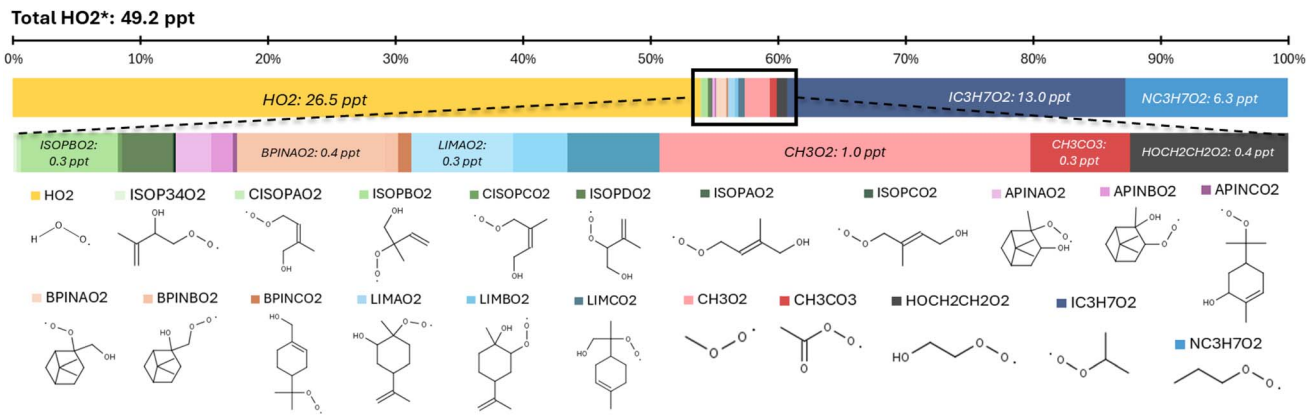

Fig. 4 The relative proportions of different HO_2 and RO_2 radicals as a contribution to the overall HO_2^* summation during the Cl-cleaning event. Species concentrations have been averaged between 17:30 and 19:30. The skeletal structures of species are also provided along with MCM names.[69,88] Structural formulae and other properties of the species can be found on the MCM webpage.[89]

(Fig. 2b), owing to the Cl-cleaning event. There was a negligible change in the HO_2^* concentration during the earlier cooking events. HO_2^* concentrations remained elevated (above the baseline of 0.7 ppt) from the Cl-cleaning began, until 19:30 where it returned to a normal level. At the peak of the HO_2^* concentration the model simulation gives about 10% higher values than the observations, well within experimental uncertainty. As described in Section 2.6, instrument interference causes some VOC-derived RO_2 radicals to be included in the HO_2 summation. INCHEM-Py enables the contribution to HO_2^* from each RO_2 derivative to be examined in detail. Fig. 4 shows the relative distribution of HO_2^* contributing species during and a short time after the cleaning period (17:30–19:30).

HO_2 represented more than half (26.5 ppt) of the total HO_2^* (49.2 ppt), comprising 54%. The two propane-derived RO_2 radicals (i-$C_3H_7O_2$ and n-$C_3H_7O_2$), comprised 19.3 ppt of the total and probably derived from a pilot light fault (Fig. 4), which also caused high indoor propane concentrations.[17] RO_2 radicals from oxidation of isoprene (0.4 ppt), α-pinene (0.2 ppt), β-pinene (0.5 ppt), limonene (0.7 ppt), ethene (0.4 ppt), the methylperoxy radical (1.0 ppt), and the acetylperoxy radical (0.3 ppt) made more minor contributions to the HO_2^* total (49.2 ppt) (Fig. 4).

For HONO (Fig. 2c and 3b) there is agreement between model (June 25 and average day) and measurements on June 8 and 25. The measurements on June 19 and 21 show trends similar to the other days, but on a higher background level of HONO equilibrium. The model outputs are compared to the CIMS measurements, which were collocated with the VOC, NO_x, and O_3 instrumentation in the kitchen. Fig. 3b shows varying background concentrations of HONO on the four days as well as differences in scatter/variation of the measurements: the CIMS instrument had lower sensitivity between June 6–17, hence the higher scatter in the data shown for June 8. However, the increases in HONO concentrations observed during cooking events (~5–6 ppb for the three main cooking events), and the sharp decrease in HONO (~5–10 ppb) during Cl-cleaning are similar on each day (Fig. 3b). The HONO decrease after the Cl-cleaning event produces similar modelled concentrations to those measured (within experimental uncertainties) for all four days (0.6–1.3 ppb) despite varying HONO concentrations before the Cl-cleaning event. Of the other types of cleaning events, only the morning cleaning event using pine sol affects the HONO concentration, with a small increase (~2 ppb) in HONO after the cleaning event.

The modelled HONO concentrations were optimised using rate coefficients for reactions (4) and (5) of $k_4 = 0.95$ cm $s^{-1} \times A_{clean}/V$ and $k_5 = 6.9 \times 10^{-4}$ s^{-1}, respectively, obtained by fitting the model to the HONO observations from June 25, and activated in the model around the time of cleaning (see Section 2). Here $A_{clean}/V = 0.16$ m^{-1}, using the area of the floor that was cleaned: $A_{clean} = 40$ m^2 and the entire UTest House volume, corresponding to $k_4 = 1.5 \times 10^{-3}$ s^{-1}. These rates have been applied in the model simulation using both the June 25 input matching the observations within the experimental uncertainty (Fig. 2c), and the average day input showing reasonable agreement (Fig. 3b). This level of agreement suggests that the reaction rate coefficients reported here can be generally applied to other Cl-cleaning events and that the HONO equilibrium between the gas-phase and cleaned surface is reasonably accounted for by reactions (4) and (5). As the Cl-cleaning impact on HONO is significantly different to the other cleaning events, we suggest that the drivers behind reactions (4) and (5) are due to the bleach solution itself and not only from the presence of a wet surface. Mattila *et al.* (2020)[33] found that aqueous uptake of HONO into a bleach-covered surface produced $ClNO_2$ could at least partly explain the gas-phase observations of both of these species. Reactions (4) and (5) described here can be used to describe the resulting impact of the heterogeneous and aqueous processes on gas-phase HONO.

The averaged day model simulated HONO is in closer agreement with the measurements on June 8 and 25 than compared to the observations on June 19 and 21. June 19 and June 21 have a higher background HONO concentration of ~12 pbb and ~8 ppb respectively compared to ~4–5 pbb for June 8 and June 25, possibly due to HONO production or off-gassing from surface films deposited during the Thanksgiving event on June 18, altering the gas-phase background steady state concentration of HONO described by the equilibrium reactions (2) and (3). Interestingly, at the time of the Cl-cleaning event all four days have HONO minimum concentration at ~1 ppb, suggesting that the cleaning event drives HONO almost to depletion in the gas-phase through reaction (4). Immediate HONO production after the Cl-cleaning suggests an additional HONO source on these days. The decrease in HONO concentration and the following rate of increase after the Cl-cleaning event, is faster for June 21 than June 8 and 25. June 19 has a gap in the data at this time, but appears to follow a similar trend to June 21 where data are available. It is not clear what is responsible for the differing behaviour on the different days, but our hypothesis is varying surface deposit composition. However, the HONO observations between the four days are all in agreement within the experimental uncertainties (Fig. 2c) and the importance of surface reservoirs for HONO (and other indoor species) is highlighted by the varying background on the different days. This is an area that warrants further study.

3.2 Predicted Cl concentrations, Cl reactivity and OH reactivity

INCHEM-Py has also been used to simulate the Cl atom concentrations, which are unable to be determined experimentally at this time. Fig. 5 shows modelled Cl atom concentration (panel a), Cl atom reactivity (panel b) and OH radical reactivity (panel c) for June 25 (grey) and the averaged day (black). The reactivity of Cl/OH is defined as the sum of the concentrations of Cl/OH reactants multiplied by the rate coefficients for that reaction. The Cl concentration is negligible before the Cl-cleaning event, peaking at 0.75×10^5 and 2.3×10^5 atom per cm^3, for the June 25 and averaged-day scenario respectively during cleaning. About an hour after the cleaning event, the Cl atoms have all been removed. The Cl atom concentration is insensitive to other activities in the house. The peak concentrations following cleaning are 1–3 orders of

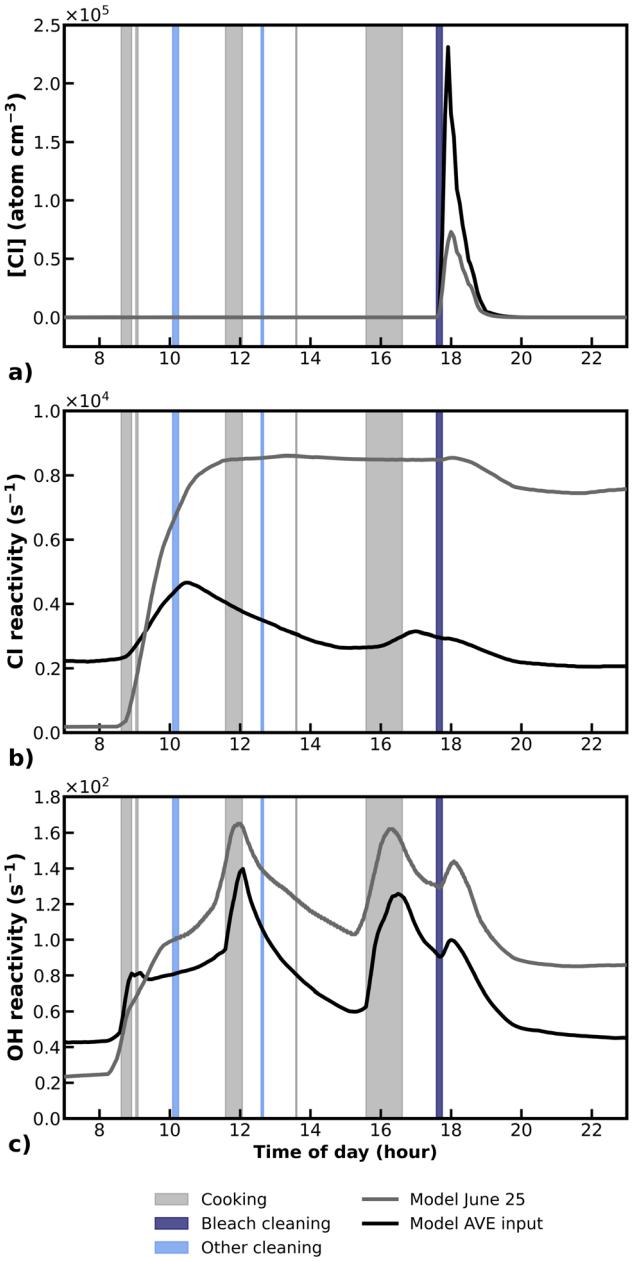

Fig. 5 Modelled Cl atom concentration (panel a, atom per cm^3), Cl atom reactivity (panel b, s^{-1}), and OH radical reactivity (panel c, s^{-1}) for the June 25 scenario (grey) and the averaged-day scenario (black). The shaded areas on each panel indicate the timing of the indoor activities carried out during the day: cooking (grey), Cl-cleaning (dark blue), and other cleaning (light blue) activities.

magnitude higher than those outdoors.[91,92] Comparing the indoor OH radical and Cl atom concentrations during and up to an hour after the Cl-cleaning event, OH radicals are about 2 orders of magnitude higher, however, Cl atoms are generally more reactive.[93,94] The combination of high Cl and OH concentrations means that the oxidative capability of the indoor air is magnified significantly.

The Cl reactivity is high, reflecting the high reactivity and generally fast oxidation reactions undertaken by Cl atoms. Fig. 5b shows the Cl reactivity increasing from a background level of about 160 and 2200 s^{-1} to a peak of around 8500 and 4800 s^{-1} for June 25 and the averaged day, respectively. The June 25 reactivity peak is maintained until the Cl-cleaning event, where it decreases slightly to about 7500 s^{-1}. On the averaged day, Cl reactivity only increases until the first cleaning event, with a second increase during the evening cooking event, eventually leveling off at about 2100 s^{-1}. The Cl reactivity profiles highlight that reactions of VOCs with Cl atoms are occurring from the time of the first cooking event, even though Cl concentrations stay low. The high reactivity of Cl atoms means that they are rapidly removed by reactions (such as with VOCs), until a significant emissions of precursor compounds (cleaning products) elevates their concentrations. This high Cl reactivity also means that chlorinated compounds (*e.g.* chlorinated organics) are likely to be formed in significant concentrations.

The OH radical reactivity presented in Fig. 5c shows increases following each of the cooking events as well as at the time of Cl-cleaning in the late afternoon. The initial background OH reactivity is between 20–40 s^{-1}, which is very similar to ambient urban observations in both London (15–27 s^{-1})[95] and Beijing (22–89 s^{-1}).[96] Following the emissions of VOCs indoors during the cooking and cleaning events, the OH reactivity increases to peaks of around 140 and 160 s^{-1} on the averaged-day and June 25 simulations, respectively. The highest peak for both model scenarios occurs after the second cooking event, higher than peak values observed during rush hour in London of 116 s^{-1}.[95] The increases following the cooking events are: 35 and 40 s^{-1} for the first event, 45 and 40 s^{-1} for the second event, and 60 and 65 s^{-1} for the third event for June 25 and the average day, respectively. After the Cl-cleaning event, an increase in OH reactivity of 10 s^{-1} is observed for both model scenarios. The similarity between these increases in reactivity, suggests that the amounts of VOCs emitted from cooking events and compounds emitted from the Cl-cleaning event are very similar for the June 25 scenario compared to the averaged day scenario. Therefore, the averaged day scenario provides a good estimate of the changes in OH reactivity from the individual activities of cooking and cleaning, even in a generalised scenario. OH reactivity can be dissected further by analysing the rates of loss of OH throughout June 25. The highest loss rate of OH was caused by the reaction with propane (27.3 ppt s^{-1}) at 17:57, which contributed approximately 76% towards the total OH loss rate and the subsequent OH reactivity. Other key loss rates for OH during Cl-cleaning include the reactions with NO and NO_2 forming HONO and HNO_3 respectively. These reactions represent approximately 3 and 12% contributions to OH reactivity during the Cl-cleaning event.

4 Conclusions

In conclusion, the observed changes in OH and HO_2^* radicals and HONO during the Cl-cleaning events of four layered days during the HOMEChem campaign in June 2018 are described well by the INCHEM-Py model. At the time of the Cl-cleaning event, OH and HO_2^* radical concentrations increased to peak

after the event and returned to background levels just over an hour later. This return to background concentrations was driven by chemical reactions, not ventilation. For instance, removal of OH by reaction with propane was 270 000 faster than removal by ventilation. HONO concentrations increase after each cooking event, and decrease at the time of Cl-cleaning. HONO slowly recovers to background concentrations several hours after the cleaning event owing to what we assume is degassing from the floor surface. Modelled Cl concentrations show a peak during and after the Cl-cleaning event, simultaneously with those in the OH and HO_2^* radical concentrations. The modelled profiles for the averaged-day and for June 25 are in general agreement, although the averaged-day simulation has higher OH and Cl concentrations during and after the Cl-cleaning event. As a comparison to the Reidy *et al.* (2023) study,[40] our data agrees well. Following cooking, the concentration of HONO increases in both studies, and OH and HO_2^* follow similar activity profiles. As an expansion to the Reidy *et al.* (2023) study,[40] we have found that the increase in OH reactivity following cooking outweighs the increase following Cl-cleaning (despite the higher OH concentration following the cleaning event).

Cl atom reactivity increases at the beginning of the day, when VOCs are being emitted through the different activities in the house and then levels out, or decreases slowly for the rest of the day. OH radical reactivity shows increases following both cooking and Cl-cleaning events, with peak levels exceeding those observed in outdoor urban environments. The increases in both Cl and OH reactivity show the impact of the oxidative capability of the indoor atmospheric environment and its dependence on the indoor activities carried out.

The addition of the HONO surface chemistry from Collins *et al.* (2018)[48] with the additional wet surface HONO chemistry described in this study, fully captures the changes in gas phase HONO during Cl-cleaning. We have described HONO wet surface chemistry by determining specific rates for the different processes following the Cl-cleaning event, providing a mechanism to be tested experimentally. The fast rate of HONO loss to a wet surface, followed by the slower degassing of HONO back to the gas phase, can be included and tested in the description of cleaning events in other indoor environments and/or other model simulations.

Data availability

Data from this project is available at **https://doi.org/10.15124/66f2972f-6d07-4a01-a8aa-583baa5ff7bd**, an online data repository hosted by the University of York.[97]

Author contributions

F. F. Ø.: conceptualization, data curation, formal analysis, investigation, methodology, validation, visualization, writing – original draft, writing – review & editing. T. J. C.: data curation, formal analysis, investigation, methodology, software, validation, visualization, writing – original draft, writing – review & editing. D. R. S.: data curation, investigation, software, supervision, writing – review & editing. J. P. D. A., A. A., C. A., B. P. B., F. J. C. S., P. F. D., D. K. F., A. H. G., L. H. R., T. F. K., J. M. M., A. N., P. S. S., E. R., C. M. F. R., C. W., S. Z.: data curation, resources, writing – review & editing. N. C.: conceptualization, funding acquisition, methodology, project administration, supervision, writing – review & editing.

Conflicts of interest

There are no conflicts to declare.

Acknowledgements

This research is part of the MOCCIE project, supported and funded by the Alfred P. Sloan Foundation through grant numbers: G-2018-10083 (D. R. S. and N. C.), G-2019-12306 (F. F. Ø. and N. C.), and G-2020-13912 (T. J. C. and N. C.). The HOMEChem project was supported and funded by the Alfred P. Sloan Foundation through grant number: G-2017-9944. The Alfred P. Sloan Foundation also supported measurements through grant number: G-2018-11061 (P. S. S., E. R., B. P. B., and C. M. F. R.). Conclusions reached or positions taken by researchers or other grantees represent the views of the grantees themselves and not those of the Alfred P. Sloan Foundation or its trustees, officers, or staff.

Notes and references

1 World Health Organisation, *WHO Global Air Quality Guidelines – Particulate Matter (PM2.5 and PM10), Ozone, Nitrogen Dioxide, Sulfur Dioxide and Carbon Monoxide*, World Health Organisation (WHO) technical report, 2021.
2 World Health Organisation, Household air pollution and health, 2023, **https://www.who.int/en/news-room/fact-sheets/detail/household-air-pollution-and-health**.
3 N. Carslaw, X. Querol, S. Nehr, S. Sousa and M. Riediker, Implementing standards for indoor air quality, 2023, **https://indairpollnet.york.ac.uk/policy-launch**.
4 L. Morawska, J. Allen, W. Bahnfleth, B. Bennett, P. M. Bluyssen, A. Boerstra, G. Buonanno, J. Cao, S. J. Dancer, A. Floto, F. Franchimon, T. Greenhalgh, C. Haworth, J. Hogeling, C. Isaxon, J. L. Jimenez, A. Kennedy, P. Kumar, J. Kurnitski, Y. Li, M. Loomans, G. Marks, L. C. Marr, L. Mazzarella, A. K. Melikov, S. L. Miller, D. K. Milton, J. Monty, P. V. Nielsen, C. Noakes, J. Peccia, K. A. Prather, X. Querol, T. Salthammer, C. Sekhar, O. Seppänen, S.-i. Tanabe, J. W. Tang, R. Tellier, K. W. Tham, P. Wargocki, A. Wierzbicka and M. Yao, Mandating indoor air quality for public buildings, *Science*, 2024, **383**, 1418–1420.
5 N. E. Klepeis, W. C. Nelson, W. R. Ott, J. P. Robinson, A. M. Tsang, P. Switzer, J. V. Behar, S. C. Hern and W. H. Engelmann, The National Human Activity Pattern Survey (NHAPS): A resource for assessing exposure to environmental pollutants, *J. Exposure Anal. Environ. Epidemiol.*, 2001, **11**, 231–252.

6 C. J. Weschler and N. Carslaw, Indoor Chemistry, *Environ. Sci. Technol.*, 2018, **52**, 2419–2428.
7 N. Carslaw, G. Bekö, S. Langer, C. Schoemaecker, V. G. Mihucz, M. Dudzinska, P. Wiesen, S. Nehr, K. Huttunen, X. Querol and D. Shaw, A new framework for indoor air chemistry measurements: Towards a better understanding of indoor air pollution, *Indoor Environ.*, 2024, **1**, 100001.
8 Y. Liu, P. K. Misztal, J. Xiong, Y. Tian, C. Arata, R. J. Weber, W. W. Nazaroff and A. H. Goldstein, Characterizing sources and emissions of volatile organic compounds in a northern California residence using space- and time-resolved measurements, *Indoor Air*, 2019, **29**, 630–644.
9 J. de Kort, F. Gauvin, M. Loomans and H. Brouwers, Emission rates of bio-based building materials, a method description for qualifying and quantifying VOC emissions, *Sci. Total Environ.*, 2023, **905**, 167158.
10 S. Guo and W. Liang, Volatile organic compounds and odor emissions characteristics of building materials and comparisons with the on-site measurements during interior construction stages, *Build. Environ.*, 2024, **252**, 111257.
11 S. B. Holøs, A. Yang, M. Lind, K. Thunshelle, P. Schild and M. Mysen, VOC emission rates in newly built and renovated buildings, and the influence of ventilation – a review and meta-analysis, *Int. J. Vent.*, 2019, **18**, 153–166.
12 D. A. Missia, E. Demetriou, N. Michael, E. I. Tolis and J. G. Bartzis, Indoor exposure from building materials: A field study, *Atmos. Environ.*, 2010, **44**, 4388–4395.
13 M. Kruza and N. Carslaw, How do breath and skin emissions impact indoor air chemistry?, *Indoor Air*, 2019, **29**, 369–379.
14 A. Wisthaler and C. J. Weschler, Reactions of ozone with human skin lipids: Sources of carbonyls, dicarbonyls, and hydroxycarbonyls in indoor air, *Proc. Natl. Acad. Sci. U. S. A.*, 2010, **107**, 6568–6575.
15 A. A. Aksenov, J. P. Koelmel, E. Z. Lin, A. V. Melnik, M. E. Vance, D. K. Farmer and K. J. Godri Pollitt, Human Activities Shape Indoor Volatile Chemistry, *Environ. Sci. Technol. Lett.*, 2023, **10**, 965–975.
16 L. Ampollini, E. F. Katz, S. Bourne, Y. Tian, A. Novoselac, A. H. Goldstein, G. Lucic, M. S. Waring and P. F. Decarlo, Observations and Contributions of Real-Time Indoor Ammonia Concentrations during HOMEChem, *Environ. Sci. Technol.*, 2019, **53**, 8591–8598.
17 D. K. Farmer, M. E. Vance, J. P. Abbatt, A. Abeleira, M. R. Alves, C. Arata, E. Boedicker, S. Bourne, F. Cardoso-Saldaña, R. Corsi, P. F. Decarlo, A. H. Goldstein, V. H. Grassian, L. Hildebrandt Ruiz, J. L. Jimenez, T. F. Kahan, E. F. Katz, J. M. Mattila, W. W. Nazaroff, A. Novoselac, R. E. O'Brien, V. W. Or, S. Patel, S. Sankhyan, P. S. Stevens, Y. Tian, M. Wade, C. Wang, S. Zhou and Y. Zhou, Overview of HOMEChem: House Observations of Microbial and Environmental Chemistry, *Environ. Sci.: Processes Impacts*, 2019, **21**, 1280–1300.
18 D. K. Farmer, M. E. Vance, D. Poppendieck, J. Abbatt, M. R. Alves, K. C. Dannemiller, C. Deeleepojananan, J. Ditto, B. Dougherty, O. R. Farinas, A. H. Goldstein, V. H. Grassian, H. Huynh, D. Kim, J. C. King, J. Kroll, J. Li, M. F. Link, L. Mael, K. Mayer, A. B. Martin, G. Morrison, R. O'Brien, S. Pandit, B. J. Turpin, M. Webb, J. Yu and S. M. Zimmerman, The chemical assessment of surfaces and air (CASA) study: using chemical and physical perturbations in a test house to investigate indoor processes, *Environ. Sci.: Processes Impacts*, 2024, 1–22, Advance Article.
19 G. Bekö, P. Wargocki, N. Wang, M. Li, C. J. Weschler, G. Morrison, S. Langer, L. Ernle, D. Licina, S. Yang, N. Zannoni and J. Williams, The Indoor Chemical Human Emissions and Reactivity (ICHEAR) project: Overview of experimental methodology and preliminary results, *Indoor Air*, 2020, **30**, 1213–1228.
20 M. Shiraiwa, N. Carslaw, D. J. Tobias, M. S. Waring, D. Rim, G. Morrison, P. S. Lakey, M. Kruza, M. Von Domaros, B. E. Cummings and Y. Won, Modelling consortium for chemistry of indoor environments (MOCCIE): Integrating chemical processes from molecular to room scales, *Environ. Sci.: Processes Impacts*, 2019, **21**, 1240–1254.
21 W. L. Brown, D. A. Day, H. Stark, D. Pagonis, J. E. Krechmer, X. Liu, D. J. Price, E. F. Katz, P. F. DeCarlo, C. G. Masoud, D. S. Wang, L. Hildebrandt Ruiz, C. Arata, D. M. Lunderberg, A. H. Goldstein, D. K. Farmer, M. E. Vance and J. L. Jimenez, Real-time organic aerosol chemical speciation in the indoor environment using extractive electrospray ionization mass spectrometry, *Indoor Air*, 2021, **31**, 141–155.
22 S. Patel, S. Sankhyan, E. K. Boedicker, P. F. Decarlo, D. K. Farmer, A. H. Goldstein, E. F. Katz, W. W. Nazaroff, Y. Tian, J. Vanhanen and M. E. Vance, Indoor Particulate Matter during HOMEChem: Concentrations, Size Distributions, and Exposures, *Environ. Sci. Technol.*, 2020, **54**, 7107–7116.
23 C. Arata, P. K. Misztal, Y. Tian, D. M. Lunderberg, K. Kristensen, A. Novoselac, M. E. Vance, D. K. Farmer, W. W. Nazaroff and A. H. Goldstein, Volatile organic compound emissions during HOMEChem, *Indoor Air*, 2021, **31**, 2099–2117.
24 C. Wang, B. Bottorff, E. Reidy, C. M. F. Rosales, D. B. Collins, A. Novoselac, D. K. Farmer, M. E. Vance, P. S. Stevens and J. P. Abbatt, Cooking, Bleach Cleaning, and Air Conditioning Strongly Impact Levels of HONO in a House, *Environ. Sci. Technol.*, 2020, **54**, 13488–13497.
25 H. L. Davies, C. O'Leary, T. Dillon, D. R. Shaw, M. Shaw, A. Mehra, G. Phillips and N. Carslaw, A measurement and modelling investigation of the indoor air chemistry following cooking activities, *Environ. Sci.: Processes Impacts*, 2023, **25**, 1532–1548.
26 M. A. Pothier, E. Boedicker, J. R. Pierce, M. Vance and D. K. Farmer, From the HOMEChem frying pan to the outdoor atmosphere: chemical composition, volatility distributions and fate of cooking aerosol, *Environ. Sci.: Processes Impacts*, 2022, **25**, 314–325.
27 S. Sankhyan, K. Zabinski, R. E. O'Brien, S. Coyan, S. Patel and M. E. Vance, Aerosol emissions and their volatility

from heating different cooking oils at multiple temperatures, *Environ. Sci.: Atmos.*, 2022, **2**, 1364–1375.

28 S. Patel, D. Rim, S. Sankhyan, A. Novoselac and M. E. Vance, Aerosol dynamics modeling of sub-500 nm particles during the HOMEChem study, *Environ. Sci.: Processes Impacts*, 2021, **23**, 1706–1717.

29 B. E. Cummings, M. A. Pothier, E. F. Katz, P. F. DeCarlo, D. K. Farmer and M. S. Waring, Model Framework for Predicting Semivolatile Organic Material Emissions Indoors from Organic Aerosol Measurements: Applications to HOMEChem Stir-Frying, *Environ. Sci. Technol.*, 2023, **57**, 17374–17383.

30 E. K. Boedicker, E. W. Emerson, G. R. McMeeking, S. Patel, M. E. Vance and D. K. Farmer, Fates and spatial variations of accumulation mode particles in a multi-zone indoor environment during the HOMEChem campaign, *Environ. Sci.: Processes Impacts*, 2021, **23**, 1029–1039.

31 B. Bottorff, C. Wang, E. Reidy, C. Rosales, D. K. Farmer, M. E. Vance, J. P. Abbatt and P. S. Stevens, Comparison of Simultaneous Measurements of Indoor Nitrous Acid: Implications for the Spatial Distribution of Indoor HONO Emissions, *Environ. Sci. Technol.*, 2022, **56**, 13573–13583.

32 C. Wang, J. M. Mattila, D. K. Farmer, C. Arata, A. H. Goldstein and J. P. Abbatt, Behavior of Isocyanic Acid and Other Nitrogen-Containing Volatile Organic Compounds in the Indoor Environment, *Environ. Sci. Technol.*, 2022, **56**, 7598–7607.

33 J. M. Mattila, P. S. Lakey, M. Shiraiwa, C. Wang, J. P. Abbatt, C. Arata, A. H. Goldstein, L. Ampollini, E. F. Katz, P. F. Decarlo, S. Zhou, T. F. Kahan, F. J. Cardoso-Saldaña, L. H. Ruiz, A. Abeleira, E. K. Boedicker, M. E. Vance and D. K. Farmer, Multiphase Chemistry Controls Inorganic Chlorinated and Nitrogenated Compounds in Indoor Air during Bleach Cleaning, *Environ. Sci. Technol.*, 2020, **54**, 1730–1739.

34 E. Harding-Smith, D. R. Shaw, M. Shaw, T. J. Dillon and N. Carslaw, Does green mean clean? Volatile organic emissions from regular versus green cleaning products, *Environ. Sci.: Processes Impacts*, 2024, **26**, 436–450.

35 J. M. Mattila, C. Arata, C. Wang, E. F. Katz, A. Abeleira, Y. Zhou, S. Zhou, A. H. Goldstein, J. P. Abbatt, P. F. Decarlo and D. K. Farmer, Dark Chemistry during Bleach Cleaning Enhances Oxidation of Organics and Secondary Organic Aerosol Production Indoors, *Environ. Sci. Technol. Lett.*, 2020, **7**, 795–801.

36 J. P. Abbatt and C. Wang, The atmospheric chemistry of indoor environments, *Environ. Sci.: Processes Impacts*, 2020, **22**, 25–48.

37 A. P. Ault, V. H. Grassian, N. Carslaw, D. B. Collins, H. Destaillats, D. J. Donaldson, D. K. Farmer, J. L. Jimenez, V. F. McNeill, G. C. Morrison, R. E. O'Brien, M. Shiraiwa, M. E. Vance, J. Wells and W. Xiong, Indoor Surface Chemistry: Developing a Molecular Picture of Reactions on Indoor Interfaces, *Chem*, 2020, **6**, 3203–3218.

38 T. J. Carter, D. G. Poppendieck, D. Shaw and N. Carslaw, A Modelling Study of Indoor Air Chemistry: The Surface Interactions of Ozone and Hydrogen Peroxide, *Atmos. Environ.*, 2023, **297**, 119598.

39 E. Harding-Smith, H. L. Davies, C. O'Leary, R. Winkless, M. Shaw, T. Dillon, B. Jones and N. Carslaw, The impact of surfaces on indoor air chemistry following cooking and cleaning, *Environ. Sci.: Processes Impacts*, 2024, 1–20, advance article.

40 E. Reidy, B. P. Bottorff, C. M. F. Rosales, F. J. Cardoso-Saldaña, C. Arata, S. Zhou, C. Wang, A. Abeleira, L. Hildebrandt Ruiz, A. H. Goldstein, A. Novoselac, T. F. Kahan, J. P. Abbatt, M. E. Vance, D. K. Farmer and P. S. Stevens, Measurements of Hydroxyl Radical Concentrations during Indoor Cooking Events: Evidence of an Unmeasured Photolytic Source of Radicals, *Environ. Sci. Technol.*, 2023, **57**, 896–908.

41 N. Zannoni, P. S. J. Lakey, Y. Won, M. Shiraiwa, D. Rim, C. J. Weschler, N. Wang, L. Ernle, M. Li, G. Bekö, P. Wargocki and J. Williams, The human oxidation field, *Science*, 2022, **377**, 1071–1077.

42 M. D. Leslie, M. Ridoli, J. G. Murphy and N. Borduas-Dedekind, Isocyanic acid (HNCO) and its fate in the atmosphere: a review, *Environ. Sci.: Processes Impacts*, 2019, **21**, 793–808.

43 F. Spataro and A. Ianniello, Sources of atmospheric nitrous acid: State of the science, current research needs, and future prospects, *J. Air Waste Manage. Assoc.*, 2014, **64**, 1232–1250.

44 S. Gligorovski, Nitrous acid (HONO): An emerging indoor pollutant, *J. Photochem. Photobiol., A*, 2016, **314**, 1–5.

45 E. G. Alvarez, D. Amedro, C. Afif, S. Gligorovski, C. Schoemacker, C. Fittschen, J. F. Doussin and H. Wortham, Unexpectedly high indoor hydroxyl radical concentrations associated with nitrous acid, *Proc. Natl. Acad. Sci. U. S. A.*, 2013, **110**, 13294–13299.

46 M. Mendez, N. Blond, D. Amedro, D. A. Hauglustaine, P. Blondeau, C. Afif, C. Fittschen and C. Schoemaecker, Assessment of indoor HONO formation mechanisms based on in situ measurements and modeling, *Indoor Air*, 2017, **27**, 443–451.

47 M. S. Waring and J. R. Wells, Volatile organic compound conversion by ozone, hydroxyl radicals, and nitrate radicals in residential indoor air: Magnitudes and impacts of oxidant sources, *Atmos. Environ.*, 2015, **106**, 382–391.

48 D. B. Collins, R. F. Hems, S. Zhou, C. Wang, E. Grignon, M. Alavy, J. A. Siegel and J. P. Abbatt, Evidence for Gas-Surface Equilibrium Control of Indoor Nitrous Acid, *Environ. Sci. Technol.*, 2018, **52**, 12419–12427.

49 C. Wang, D. B. Collins, C. Arata, A. H. Goldstein, J. M. Mattila, D. K. Farmer, L. Ampollini, P. F. DeCarlo, A. Novoselac, M. E. Vance, W. W. Nazaroff and J. P. D. Abbatt, Surface reservoirs dominate dynamic gas-surface partitioning of many indoor air constituents, *Sci. Adv.*, 2020, **6**, 8973.

50 D. Shaw and N. Carslaw, INCHEM-Py: An open source Python box model for indoor air chemistry, *J. Open Source Softw.*, 2021, **6**, 3224.

51 D. R. Shaw, T. J. Carter, H. L. Davies, E. Harding-Smith, E. C. Crocker, G. Beel, Z. Wang and N. Carslaw, INCHEM-Py v1.2: a community box model for indoor air chemistry, *Geosci. Model Dev.*, 2023, **16**, 7411–7431.

52 N. Carslaw, A mechanistic study of limonene oxidation products and pathways following cleaning activities, *Atmos. Environ.*, 2013, **80**, 507–513.

53 N. Carslaw, L. Fletcher, D. Heard, T. Ingham and H. Walker, Significant OH production under surface cleaning and air cleaning conditions: Impact on indoor air quality, *Indoor Air*, 2017, **27**, 1091–1100.

54 J. P. Wong, N. Carslaw, R. Zhao, S. Zhou and J. P. Abbatt, Observations and impacts of bleach washing on indoor chlorine chemistry, *Indoor Air*, 2017, **27**, 1082–1090.

55 A. M. Yeoman, M. Shaw, N. Carslaw, T. Murrells, N. Passant and A. C. Lewis, Simplified speciation and atmospheric volatile organic compound emission rates from non-aerosol personal care products, *Indoor Air*, 2020, **30**, 459–472.

56 A. M. Yeoman, M. Shaw and A. C. Lewis, Estimating person-to-person variability in VOC emissions from personal care products used during showering, *Indoor Air*, 2021, **31**, 1281–1291.

57 S. Zhou, Z. Liu, Z. Wang, C. J. Young, T. C. Vandenboer, B. B. Guo, J. Zhang, N. Carslaw and T. F. Kahan, Hydrogen Peroxide Emission and Fate Indoors during Non-bleach Cleaning: A Chamber and Modeling Study, *Environ. Sci. Technol.*, 2020, **54**, 15643–15651.

58 P. S. Lakey, Y. Won, D. Shaw, F. F. Østerstrøm, J. Mattila, E. Reidy, B. Bottorff, C. Rosales, C. Wang, L. Ampollini, S. Zhou, A. Novoselac, T. F. Kahan, P. F. DeCarlo, J. P. Abbatt, P. S. Stevens, D. K. Farmer, N. Carslaw, D. Rim and M. Shiraiwa, Spatial and temporal scales of variability for indoor air constituents, *Commun. Chem.*, 2021, **4**, 1–7.

59 N. Carslaw and D. Shaw, Modification of cleaning product formulations could improve indoor air quality, *Indoor Air*, 2022, **32**, 1–13.

60 M. Kruza, A. C. Lewis, G. C. Morrison and N. Carslaw, Impact of surface ozone interactions on indoor air chemistry: A modeling study, *Indoor Air*, 2017, **27**, 1001–1011.

61 M. Kruza, D. Shaw, J. Shaw and N. Carslaw, Towards improved models for indoor air chemistry: A Monte Carlo simulation study, *Atmos. Environ.*, 2021, **262**, 118625.

62 G. Beel, B. Langford, N. Carslaw, D. Shaw and N. Cowan, Temperature driven variations in VOC emissions from plastic products and their fate indoors: A chamber experiment and modelling study, *Sci. Total Environ.*, 2023, **881**, 163497.

63 T. J. Carter, D. R. Shaw, D. C. Carslaw and N. Carslaw, Indoor cooking and cleaning as a source of outdoor air pollution in urban environments, *Environ. Sci.: Processes Impacts*, 2024, **26**, 975–990.

64 Z. Wang, S. F. Kowal, N. Carslaw and T. F. Kahan, Photolysis-driven indoor air chemistry following cleaning of hospital wards, *Indoor Air*, 2020, **30**, 1241–1255.

65 Z. Wang, D. Shaw, T. Kahan, C. Schoemaecker and N. Carslaw, A modeling study of the impact of photolysis on indoor air quality, *Indoor Air*, 2022, **32**, 1–10.

66 N. Carslaw, T. Mota, M. E. Jenkin, M. H. Barley and G. McFiggans, A Significant role for nitrate and peroxide groups on indoor secondary organic aerosol, *Environ. Sci. Technol.*, 2012, **46**, 9290–9298.

67 N. Carslaw, M. Ashmore, A. C. Terry and D. C. Carslaw, Crucial Role for Outdoor Chemistry in Ultrafine Particle Formation in Modern Office Buildings, *Environ. Sci. Technol.*, 2015, **49**, 11011–11018.

68 M. Kruza, G. McFiggans, M. S. Waring, J. R. Wells and N. Carslaw, Indoor secondary organic aerosols: Towards an improved representation of their formation and composition in models, *Atmos. Environ.*, 2020, **240**, 117784.

69 M. E. Jenkin, S. M. Saunders and M. J. Pilling, The tropospheric degradation of volatile organic compounds: A protocol for mechanism development, *Atmos. Environ.*, 1997, **31**, 81–104.

70 M. E. Jenkin, S. M. Saunders, V. Wagner and M. J. Pilling, Protocol for the development of the Master Chemical Mechanism, MCM v3 (Part B): tropospheric degradation of aromatic volatile organic compounds, *Atmos. Chem. Phys.*, 2003, **3**, 181–193.

71 L. K. Xue, S. M. Saunders, T. Wang, R. Gao, X. F. Wang, Q. Z. Zhang and W. X. Wang, Development of a chlorine chemistry module for the Master Chemical Mechanism, *Geosci. Model Dev.*, 2015, **8**, 3151–3162.

72 M. E. Jenkin, K. P. Wyche, C. J. Evans, T. Carr, P. S. Monks, M. R. Alfarra, M. H. Barley, G. B. McFiggans, J. C. Young and A. R. Rickard, Development and chamber evaluation of the MCM v3.2 degradation scheme for β-caryophyllene, *Atmos. Chem. Phys.*, 2012, **12**, 5275–5308.

73 M. E. Jenkin, J. C. Young and A. R. Rickard, The MCM v3.3.1 degradation scheme for isoprene, *Atmos. Chem. Phys.*, 2015, **15**, 11433–11459.

74 S. M. Saunders, M. E. Jenkin, R. G. Derwent and M. J. Pilling, Protocol for the development of the Master Chemical Mechanism, MCM v3 (Part A): Tropospheric degradation of non-aromatic volatile organic compounds, *Atmos. Chem. Phys.*, 2003, **3**, 161–180.

75 C. Bloss, V. Wagner, M. E. Jenkin, R. Volkamer, W. J. Bloss, J. D. Lee, D. E. Heard, K. Wirtz, M. Martin-Reviejo, G. Rea, J. C. Wenger and M. J. Pilling, Development of a detailed chemical mechanism (MCMv3.1) for the atmospheric oxidation of aromatic hydrocarbons, *Atmos. Chem. Phys.*, 2005, **5**, 641–664.

76 S. Zhou and T. F. Kahan, Spatiotemporal characterization of irradiance and photolysis rate constants of indoor gas-phase species in the UTest house during HOMEChem, *Indoor Air*, 2022, **32**, 1–11.

77 P. Brophy and D. K. Farmer, Clustering, methodology, and mechanistic insights into acetate chemical ionization using high-resolution time-of-flight mass spectrometry, *Atmos. Meas. Tech.*, 2016, **9**, 3969–3986.

78 B. Bottorff, E. Reidy, L. Mielke, S. Dusanter and P. S. Stevens, Development of a laser-photofragmentation laser-induced fluorescence instrument for the detection of nitrous acid and hydroxyl radicals in the atmosphere, *Atmos. Meas. Tech.*, 2021, **14**, 6039–6056.

79 R. Holzinger, PTRwid: A new widget tool for processing PTR-TOF-MS data, *Atmos. Meas. Tech.*, 2015, **8**, 3903–3922.
80 A. Abeleira, I. B. Pollack, B. Sive, Y. Zhou, E. V. Fischer and D. K. Farmer, Source characterization of volatile organic compounds in the Colorado Northern Front Range Metropolitan Area during spring and summer 2015, *J. Geophys. Res.*, 2017, **122**, 3595–3613.
81 P. Brophy and D. K. Farmer, A switchable reagent ion high resolution time-of-flight chemical ionization mass spectrometer for real-time measurement of gas phase oxidized species: Characterization from the 2013 southern oxidant and aerosol study, *Atmos. Meas. Tech.*, 2015, **8**, 2945–2959.
82 P. L. Kebabian, E. C. Wood, S. C. Herndon and A. Freedman, A practical alternative to chemiluminescence-based detection of nitrogen dioxide: Cavity attenuated phase shift spectroscopy, *Environ. Sci. Technol.*, 2008, **42**, 6040–6045.
83 J. D. Goetz, A. Avery, B. Werden, C. Floerchinger, E. C. Fortner, J. Wormhoudt, P. Massoli, S. C. Herndon, C. E. Kolb, W. B. Knighton, J. Peischl, C. Warneke, J. A. De Gouw, S. L. Shaw and P. F. DeCarlo, Analysis of local-scale background concentrations of methane and other gas-phase species in the Marcellus Shale, *Elem. Sci. Anth.*, 2017, **5**, 1–20.
84 N. Carslaw, A new detailed chemical model for indoor air pollution, *Atmos. Environ.*, 2007, **41**, 1164–1179.
85 F. Vichi, L. Mašková, M. Frattoni, A. Imperiali and J. Smolík, Simultaneous measurement of nitrous acid, nitric acid, and nitrogen dioxide by means of a novel multipollutant diffusive sampler in libraries and archives, *Heritage Sci.*, 2016, **4**, 4.
86 A. Manuja, J. Ritchie, K. Buch, Y. Wu, C. M. Eichler, J. C. Little and L. C. Marr, Total surface area in indoor environments, *Environ. Sci.: Processes Impacts*, 2019, **21**, 1384–1392.
87 M. M. Lew, S. Dusanter and P. S. Stevens, Measurement of interferences associated with the detection of the hydroperoxy radical in the atmosphere using laser-induced fluorescence, *Atmos. Meas. Tech.*, 2018, **11**, 95–109.
88 M. E. Jenkin, S. M. Saunders, V. Wagner and M. J. Pilling, Protocol for the development of the Master Chemical Mechanism, MCM v3 (Part B): tropospheric degradation of aromatic volatile organic compounds, *Atmos. Sci.*, 2003, **3**, 181–193.
89 Master Chemical Mechanism, MCM v3.3.1, 2024, **https://mcm.york.ac.uk/MCM/browse**, Date Accessed: November 2024.
90 M. Li, E. Karu, C. Brenninkmeijer, H. Fischer, J. Lelieveld and J. Williams, Tropospheric OH and stratospheric OH and Cl concentrations determined from CH_4, CH_3Cl, and SF_6 measurements, *npj Clim. Atmos. Sci.*, 2018, **1**, 29.
91 B. J. Finlayson-Pitts and J. N. Pitts Jr, *Chemistry of the Upper and Lower Atmosphere*, Academic Press, San Diego, 2000.
92 W. Allan, H. Struthers, D. C. Lowe and S. E. Mikaloff Fletcher, Modeling the effects of methane source changes on the seasonal cycles of methane mixing ratio and ^{13}C in Southern Hemisphere midlatitudes, *J. Geophys. Res.:Atmos.*, 2010, **115**, 1–8.
93 R. Atkinson, D. L. Baulch, R. A. Cox, J. N. Crowley, R. F. Hampson, R. G. Hynes, M. E. Jenkin, M. J. Rossi and J. Troe, Evaluated kinetic and photochemical data for atmospheric chemistry: Volume I - gas phase reactions of Ox, HOx, NOx and SOx species, *Atmos. Chem. Phys.*, 2004, **4**, 1461–1738.
94 R. Atkinson, D. L. Baulch, R. A. Cox, J. N. Crowley, R. F. Hampson, R. G. Hynes, M. E. Jenkin, M. J. Rossi and J. Troe, Evaluated kinetic and photochemical data for atmospheric chemistry: Volume II – gas phase reactions of organic species, *Atmos. Chem. Phys.*, 2006, **6**, 3625–4055.
95 L. K. Whalley, D. Stone, B. Bandy, R. Dunmore, J. F. Hamilton, J. Hopkins, J. D. Lee, A. C. Lewis and D. E. Heard, Atmospheric OH reactivity in central London: Observations, model predictions and estimates of in situ ozone production, *Atmos. Chem. Phys.*, 2016, **16**, 2109–2122.
96 L. K. Whalley, E. J. Slater, R. Woodward-Massey, C. Ye, J. D. Lee, F. Squires, J. R. Hopkins, R. E. Dunmore, M. Shaw, J. F. Hamilton, A. C. Lewis, A. Mehra, S. D. Worrall, A. Bacak, T. J. Bannan, H. Coe, C. J. Percival, B. Ouyang, R. L. Jones, L. R. Crilley, L. J. Kramer, W. J. Bloss, T. Vu, S. Kotthaus, S. Grimmond, Y. Sun, W. Xu, S. Yue, L. Ren, W. Joe, C. Nicholas Hewitt, X. Wang, P. Fu and D. E. Heard, Evaluating the sensitivity of radical chemistry and ozone formation to ambient VOCs and NOx in Beijing, *Atmos. Chem. Phys.*, 2021, **21**, 2125–2147.
97 F. Østerstrøm, T. J. Carter, D. R. Shaw and N. Carslaw, Dataset for Modelling Indoor Radical Chemistry during the HOMEChem Campaign, 2024, DOI: **10.15124/66f2972f-6d07-4a01-a8aa-583baa5ff7bd**.